文章编号：1001-9014(XXXX)XX-0001-18

DOI：10. 11972/j. issn. 1001-9014. JIMW. 2026173

Infrared gas sensing technologies from established approaches to emerging frontiers

Wu Hai-Tao[1,2,3], Hang Rui[1,3], Li Qing[1,2,3*], Hu Wei-Da[1,2,3]

(1. School of Physics and Optoelectronic Engineering, Hangzhou Institute for Advanced Study, University of Chinese Academy of Sciences, Hangzhou 310024, China;
2. State Key Laboratory of Infrared Physics, Shanghai Institute of Technical Physics, Chinese Academy of Sciences, Shanghai 200083, China;
3. University of Chinese Academy of Sciences, Beijing 100049, China.)

Abstract: Infrared gas sensing, based on the characteristic infrared absorption of gas molecules, provides an optical approach for gas identification and concentration quantification. It has found broad applications in environmental monitoring, industrial safety, breath analysis, remote sensing, and other fields. Driven by the growing demand for miniaturized, integrated, and multi-component detection systems, the performance of infrared gas sensors is no longer determined by individual device optimization alone, but increasingly depends on the coordinated design of light sources, gas-light interaction structures, detectors, and spectral models. This review summarizes recent advances in infrared gas sensing from the perspective of system-level design and key enabling technologies. The evolution of light sources from broadband incoherent emitters to lasers and frequency combs is first discussed. Gas-light interaction structures, including free-space gas cells, hollow-core fibers, and on-chip waveguides, are then reviewed. Detector technologies are summarized in terms of photon, thermal, and photoacoustic detection mechanisms. In addition, spectral modeling methods for information extraction, including sampling optimization, multivariate regression, and machine learning, are discussed. Finally, future directions toward high sensitivity, multi-component analysis, miniaturization, intelligent sensing, and on-chip integration are outlined.

Key words: infrared gas sensing, molecular absorption spectroscopy, device integration, spectral modeling, intelligent spectral retrieval

Introduction

Infrared gas sensing is an optical detection technology that enables gas identification and concentration quantification based on the characteristic infrared absorption of gas molecules[1-2]. Gas molecules exhibit distinct absorption features in the infrared region arising from vibrational and rotational energy-level transitions, allowing infrared absorption spectroscopy to provide high molecular selectivity, real-time response, and quantitative capability. In particular, in the mid-infrared region (2-20 μm)[3-7], most gas molecules possess strong fundamental absorption bands, whose absorption intensities are typically much higher than those of overtone and combination bands in the near-infrared region. This makes mid-infrared gas sensing especially advantageous for trace gas detection[8-15], complex mixture analysis[16-20], and in situ monitoring[21-23]. After decades of development, infrared gas sensing has expanded from conventional laboratory spectroscopic instruments to diverse platforms, including atmospheric remote sensing[24-25], open-path monitoring[26-27], industrial field detection[28], portable sensors[29-32], and on-chip integrated devices[33-36]. It has become an important interdisciplinary field that integrates molecular spectroscopy, optoelectronic devices, micro- and nanophotonics, and data analysis methods.

The development of infrared gas sensing is essentially driven by the continuous optimization of key performance metrics, including sensitivity, selectivity, response speed, system size, cost, and stability. Techniques such as Fourier-transform infrared spectroscopy and tunable diode laser absorption spectroscopy[37-38] can provide high spectral resolution and high-precision analytical capability. However, they often rely on complex optical configurations, high-performance light sources[39-41], long-path gas cells[42-45], or highly sensitive detectors[46-48], which limits their use in miniaturized, low-cost, and distributed sensing applications. Meanwhile, practical sensing systems are still challenged by weak trace absorption signals[49-51], spectral overlap among multiple gas species[52], complex background interference, and insufficient long-term stability[53]. These issues cre-

Foundation items: supported by the National Natural Science Foundation of China (62522503, 62375059 and U24A20308), the Zhejiang Provincial Natural Science Foundation of China (LZ25F040001), the Hangzhou Natural Science Foundation (2025SZRJJ2055), and the Research Funds of Hangzhou Institute for Advanced Study, UCAS

* **Corresponding author**: E-mail: liqing@ucas. ac. cn

ate intrinsic trade-offs among sensitivity, selectivity, integration level, and application adaptability. Therefore, achieving highly sensitive, selective, and stable gas detection under constraints of limited volume, power consumption, and spectral resources remains a central challenge in this field.

To address these challenges, infrared gas sensing technologies have evolved rapidly in recent years in terms of light sources, light-gas interaction, signal detection, and data interpretation. Emerging infrared light sources[54], high-performance detectors[46-47], and low-noise readout techniques[55-57] have continuously improved the signal-to-noise ratio (SNR) and spectral resolving capability of sensing systems. Multi-pass gas cells, hollow-core fibers[58-59], micro- and nanowaveguides, and on-chip photonic devices have extended the effective optical path length and expanded the spatial scales of gas sensing[60]. Meanwhile, spectral modeling methods, including sampling optimization, multivariate inversion[61], and machine learning[62-63], have provided new approaches for information extraction in low-resolution, few-channel, and multi-component detection scenarios. These advances indicate that performance improvement in infrared gas sensing is shifting from the optimization of individual devices toward the coordinated design of hardware structures, spectral information, and algorithmic models.

This review aims to provide a systematic overview of infrared gas sensing from the perspectives of technological evolution and system performance. First, the fundamental principles, system architecture, and key performance metrics of infrared gas sensing are introduced. Then, recent progress in key components and methodologies, including light sources, gas interaction structures, detectors, and spectral models, is discussed, with emphasis on their technical features and applicable scenarios. Finally, representative infrared gas sensing technologies are comprehensively compared in terms of detection limits, operating spectral regions, and effective optical path lengths, so as to evaluate their sensitivity levels, system scales, and application adaptability. Future trends toward high sensitivity, multi-component detection, miniaturization, intelligent sensing, and on-chip integration are further discussed.

1 Principles, architecture, and metrics

The physical basis of infrared gas sensing is the selective absorption of infrared light by gas molecules at specific wavelengths. When the frequency of incident light matches the vibrational or rotational energy-level transitions of a gas molecule, part of the optical energy is absorbed, producing characteristic absorption features in the transmission spectrum. For a single absorbing gas, under ideal conditions, the transmitted light intensity can be described by the Beer-Lambert law:

$$I = I_0 \quad xp(-kLx), \tag{1}$$

where I_0 is the incident light intensity, I is the transmitted light intensity, k is the absorption coefficient, L is the effective optical path length, and x is the gas concentration. This relationship indicates that the infrared absorption signal is jointly determined by the incident optical intensity, molecular absorption strength, light-gas interaction length, and gas concentration. Therefore, improving the performance of infrared gas sensing does not rely on a single parameter, but requires systematic optimization of spectral acquisition, path-length enhancement, signal readout, and concentration retrieval.

Based on this fundamental relationship, an infrared gas sensing system can be understood from four key aspects, as illustrated in Fig. 1. First, the infrared light source determines the accessible spectral range, incident optical power, and spectral resolving capability. Broadband incoherent sources are suitable for low-cost and multi-band detection, laser sources enable highly selective detection targeting specific absorption lines, and frequency combs provide both broad spectral coverage and precise frequency references. Second, the light-gas interaction structure determines the effective optical path length and the spatial scale of the system. Free-space gas cells can enhance absorption signals through multi-pass reflection, hollow-core fibers can extend the light-gas interaction path within a compact volume, and on-chip waveguides further push gas sensing toward the chip scale. Third, infrared detectors convert absorption-induced optical changes into measurable signals, and their response mechanisms and noise characteristics directly affect the detection limit, response speed, and applicable spectral range. Finally, spectral models determine how gas species and concentration information can be extracted from limited, overlapping, or noisy measurement signals, which is particularly important for low-resolution, few-channel, and multi-component detection.

Therefore, infrared gas sensing can be regarded as an integrated system composed of light sources, gas cells, detectors, and spectral models. These four elements correspond, respectively, to the incident optical intensity, absorption path, output signal, and concentration retrieval process in the Beer-Lambert framework, and together determine the sensitivity, selectivity, integration level, and application adaptability of the system. The framework shown in Fig. 1 also forms the main structure of this review. The following sections will discuss the development of infrared gas sensing technologies from mature methods to emerging directions, focusing on infrared light sources, gas interaction structures, infrared detectors, and spectral models.

2 Light sources: spectral generation

The light source is the starting point of an infrared gas sensing system, determining the accessible spectral range, optical power, modulation scheme, spectral resolution, and system complexity. For absorption-based sensing governed by the Beer-Lambert law, the light source not only affects the incident optical intensity I_0, but also determines what type of molecular absorption information can be acquired by the system. According to their emission characteristics and operating mechanisms, light sources used in infrared gas sensing can be broadly classified into incoherent broadband sources, semicon-

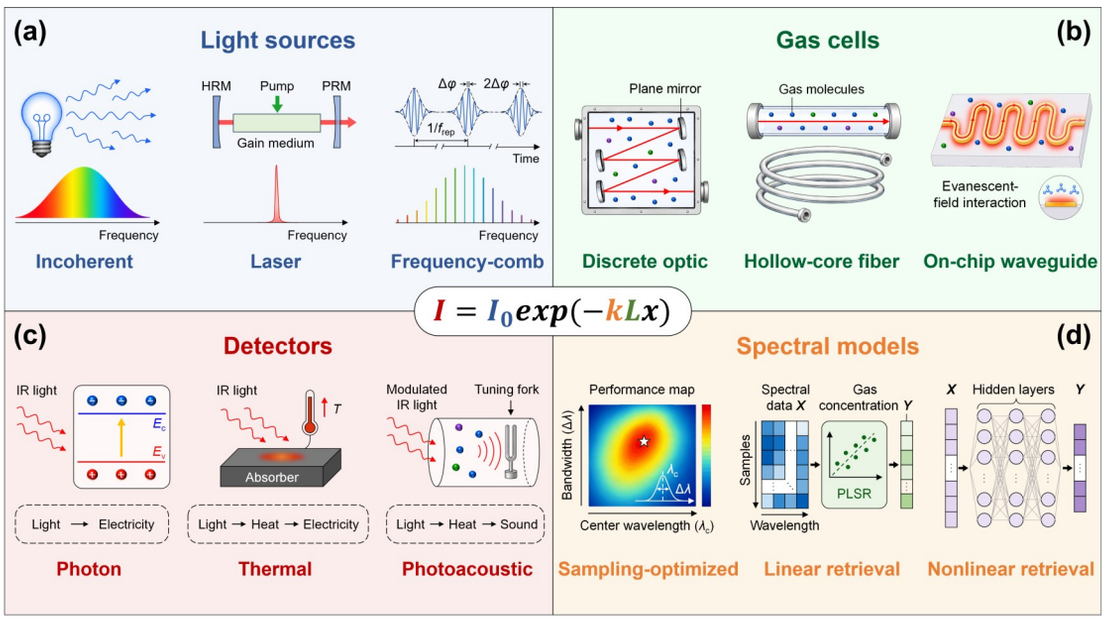

Fig. 1 Key optimization directions in infrared gas sensing technologies: (a) Infrared light sources for providing molecular absorption information; (b) Gas interaction structures for enhancing the effective optical path length; (c) Infrared detectors for converting absorption-induced signals into measurable outputs; (d) Spectral models for optimizing spectral sampling and retrieving gas species and concentrations

图 1 红外气体传感技术中的关键优化方向:(a) 红外光源,用于提供分子吸收信息;(b) 气体相互作用结构,用于增强有效光程;(c) 红外探测器,用于将吸收引起的信号转化为可测量输出;(d) 光谱模型,用于优化光谱采样并反演气体种类和浓度

ductor light-emitting devices, laser sources, and frequency comb sources. These categories correspond to different technical routes, including broadband spectral coverage, low-power integration, highly selective detection, and precise multi-component analysis. Fig. 2 summarizes representative advances in these light-source technologies for infrared gas sensing.

Incoherent thermal radiation sources are the most commonly used light sources in non-dispersive infrared (NDIR) gas sensing, owing to their broadband emission, low cost, and simple structure. Although conventional miniature lamps and micro-electro-mechanical systems (MEMS) thermal emitters have been widely used, their performance can still be limited by modulation frequency, spectral coverage, and system integration. Broadband infrared sources based on super-aligned carbon nanotube films[64] provide a promising alternative. As shown in Fig. 2(a), such films can serve as compact infrared emitters, with an emission spectrum covering 0.2 – 334 μm and a high average emissivity in the mid-infrared range of 2 – 25 μm. Owing to the fast electro-thermal response of carbon nanotube films, this type of source enables electronic modulation with modulation frequencies up to approximately 150 kHz, thereby reducing the dependence on mechanical choppers. Fig. 2(b) further demonstrates its application in human-exhaled CO_2 detection. These studies indicate that the development of incoherent infrared sources is no longer limited to increasing radiated power, but is moving toward high emissivity, fast electrical modulation, and easy integration, offering a new source platform for miniaturized, multi-gas, and fast-response NDIR sensing.

Semiconductor light-emitting devices generally feature low power consumption, compact size, and strong integration potential. However, the emission wavelengths of conventional infrared light-emitting diodes (LEDs) are usually fixed after fabrication, making it difficult to meet the multi-band matching requirements of multi-gas detection. Strain-tunable black phosphorus (BP) LEDs[65] represent a new strategy for source-level spectral control. Taking advantage of the high strain sensitivity of the BP bandgap, the photoluminescence peak can be continuously tuned over the range of 2.3 – 5.5 μm, while the electroluminescence peak of BP-MoS_2 heterojunction LEDs can be tuned from 2.70 to 4.07 μm. As shown in Fig. 2(c), the emission spectrum of BP devices can be actively controlled by tensile or compressive strain, and Fig. 2(d) demonstrates the application of this tunable LED in CO_2 and CH_4 detection. Unlike the conventional scheme of "broadband source plus optical filter," this approach matches gas absorption bands by directly tuning the emission spectrum of the light source itself, reflecting the evolution of infrared semiconductor sources from fixed-wavelength emission toward actively tunable emission.

Laser sources are characterized by narrow linewidth, high brightness, and good wavelength tunability, enabling highly selective and sensitive detection of specific molecular absorption lines. Among them, tunable diode laser absorption spectroscopy (TDLAS) is a representative high-performance approach in infrared gas sensing. As shown in Fig. 2(e)-(g), a methane tunable diode laser absorption spectroscopy system based on a 1.65 μm distributed-feedback (DFB) laser scans the

CH_4 absorption line near 6050 cm^{-1} using a 30 m multi-pass cell, achieving methane detection over the range of 1 – 100 ppm. The system further combines a Transformer-based denoising network with a multilayer perceptron[66] to realize end-to-end concentration prediction from noisy transmission spectra, improving retrieval stability under low-concentration conditions. This type of work demonstrates the advantages of laser sources in absorption-line selection, high-resolution measurement, and concentration quantification. It also indicates that laser-based gas sensing is increasingly moving toward the coordinated optimization of light sources, optical paths, noise suppression, and intelligent retrieval.

Frequency comb sources combine broad spectral coverage, narrow-linewidth comb teeth, and precise frequency references, making them an important platform for simultaneous multi-component detection in complex gas mixtures. As shown in Fig. 2(h), mid-infrared frequency combs can be combined with high-finesse optical cavities and interferometric readout structures to achieve high-resolution gas detection over a broad spectral range. A representative modulated ring-down frequency-comb interferometry system[67] covers two mid-infrared regions, 1850 – 2230 cm^{-1} and 2700 – 3330 cm^{-1}, and achieves cavity finesses of approximately 23,000 and 14,000 in the 5 μm and 3 μm bands, respectively. Fig. 2(i) shows representative spectral results obtained from interferogram processing of breath samples, where the Fourier components corresponding to different cavity resonances can be used to extract ring-down times. This system further enables simultaneous quantification of 20 molecular species in breath and ambient air with ppt-level detection sensitivity, highlighting the frontier capability of frequency comb sources in broadband, high-resolution, high-dynamic-range, and complex molecular fingerprint analysis.

Overall, the development of infrared light sources reflects a transition from simply "providing sufficient optical power" to "providing high-quality spectral information." Incoherent thermal sources are well suited for low-cost and compact NDIR systems; tunable semiconductor sources emphasize low power consumption and source-level spectral control; laser sources achieve highly selective detection through narrow linewidth and wavelength tunability, and are increasingly being integrated with intelligent algorithms; frequency comb sources are oriented toward broadband, high-resolution, and simultaneous multi-component analysis. In the future, infrared light sources for gas sensing will continue to evolve toward broader spectral coverage, low-power modulation, wavelength tunability, system integration, and more efficient use of spectral information.

3 Gas interaction: path-length engineering

Gas interaction structures determine the interaction length, interaction volume, and spatial scale between infrared light and target gas molecules, and therefore play a crucial role in sensing sensitivity and system configuration. According to the Beer-Lambert law, increasing the effective optical path length can enhance the absorption signal. However, this often comes at the cost of increased system volume, more complex optical alignment, higher coupling loss, and longer response time. Therefore, the central challenge in the development of gas interaction structures is how to enhance light-gas interaction within a limited space while maintaining stability, compactness, and integrability. Fig. 3 summarizes several representative structures, illustrating the evolution of infrared gas interaction platforms from free-space gas cells to hollow waveguides, hollow-core fibers, and on-chip waveguides.

Discrete optical gas cells are the most classical interaction structures in infrared gas sensing. Single-pass cells are simple in configuration but provide limited optical path length, whereas multi-pass cells can significantly extend the path length through repeated mirror reflections, usually at the expense of larger volume and precise optical alignment. In addition to regular reflective optical paths, integrating-sphere structures based on diffuse reflection offer a new approach for compact long-path sensing. As shown in Fig. 3(a), a rotating integrating-sphere gas cell[68] uses a highly reflective inner wall to scatter infrared light multiple times inside the sphere, achieving an equivalent optical path length of approximately 66 cm within a compact volume. Its cross-sectional structure further shows that the light source, gas inlet and outlet, and multiple filter channels can be arranged around the sphere. Fig. 3(b) demonstrates the mixed-gas detection process, in which different filter channels sequentially respond to components such as CH_4, N_2O, and C_2H_4 through mechanical rotation. Fig. 3(c) presents the detection limits for multiple gases, indicating that this type of structure can not only enhance optical path length but also support multi-channel NDIR detection and gas mixture analysis. These results suggest that discrete optical gas cells are evolving from simple path-length enhancement toward multi-channel integration, system simplification, and mixture reconstruction.

Hollow waveguides further combine the optical transmission path and gas absorption space into a single structure, providing an important route toward compact infrared gas sensing. Compared with free-space multi-pass cells, hollow waveguides can provide meter-scale absorption paths within a small volume, while offering advantages such as simple configuration, mechanical flexibility, fast response, and ease of board-level integration. As shown in Fig. 3(d), a typical board-level sensing system employs an AgI/Ag-coated flexible hollow waveguide[69] as the CO_2 absorption cell, with the light source, driving circuit, gas flow path, and detector integrated on a compact substrate. In this system, a 1 m long hollow waveguide is coiled within a board-level volume of approximately 180×100×10 mm^3, achieving CO_2 detection limits of approximately 174 ppb and 263 ppb under straight and coiled waveguide configurations, respectively. Fig. 3(e) shows the absorption spectra at different CO_2 concentrations, where the mid-infrared absorption

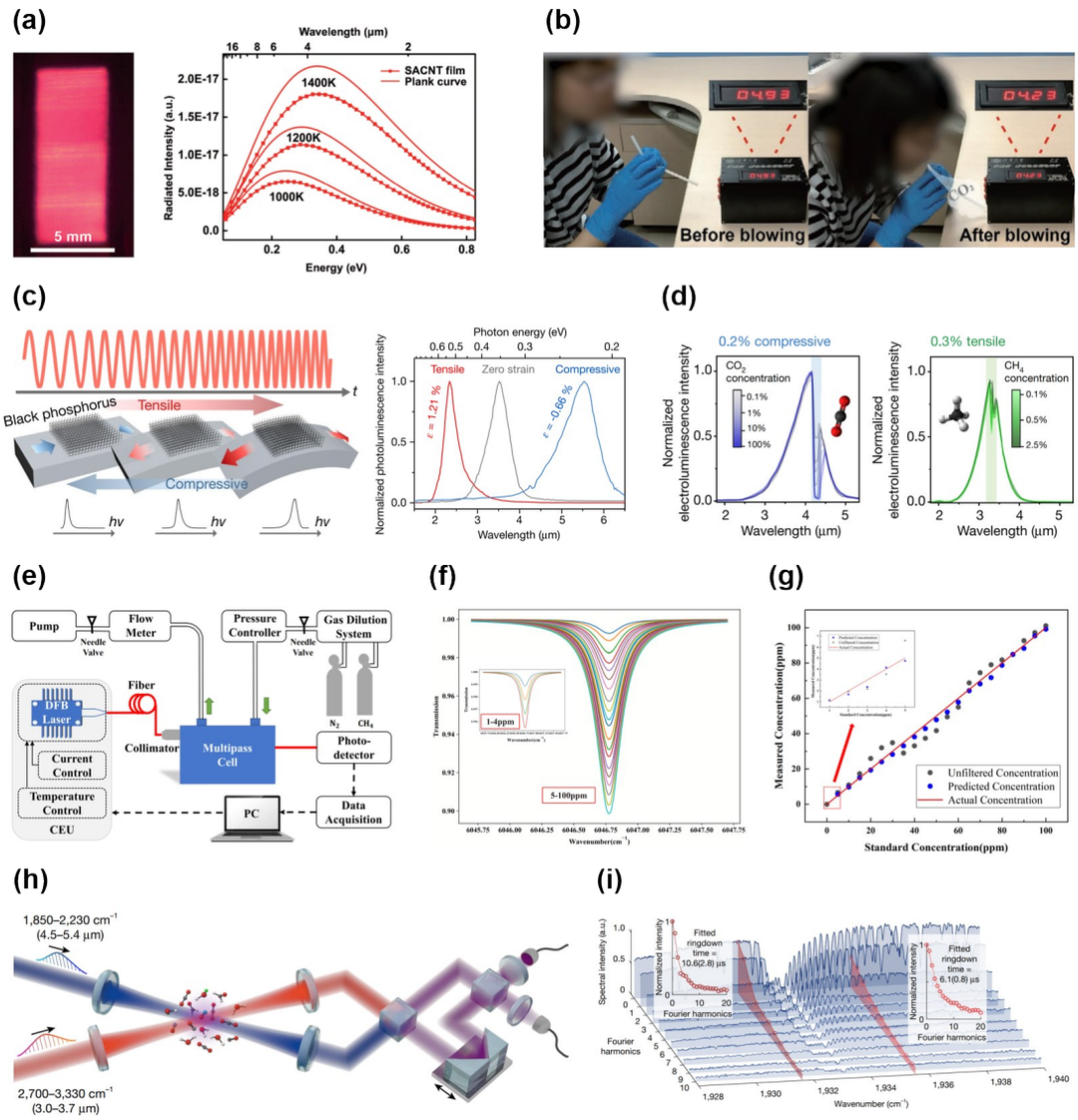

Fig. 2　Representative infrared light sources for gas sensing: (a), (b) Super-aligned carbon nanotube film broadband infrared source, including the source image, temperature-dependent emission spectra, and exhaled CO_2 detection demonstration[64]; (c), (d) Strain-tunable BP mid-infrared LED, including its operating principle, strain-dependent emission spectra, and CO_2/CH_4 sensing results[65]; (e)-(g) DFB-laser-based TDLAS system for methane detection, including the experimental setup, concentration-dependent spectra, and comparison between standard and measured concentrations[66]; (h), (i) Mid-infrared frequency-comb spectroscopy, including the gas detection configuration and spectral data processed from breath-sample interferograms for ringdown-time extraction[67]

图 2　气体传感中的代表性红外光源：(a), (b) 超顺排碳纳米管薄膜宽谱红外光源,包括光源图像、温度相关发射光谱以及呼出 CO2 检测演示[64];(c), (d) 应变可调谐 BP 中红外 LED,包括其工作原理、应变相关发射光谱以及 CO2/CH4 传感结果[65];(e)-(g) 基于 DFB 激光器的甲烷 TDLAS 系统,包括实验装置、浓度相关光谱以及标准浓度与测量浓度的对比[66];(h), (i) 中红外频率梳光谱,包括气体检测结构以及由呼气样品干涉图处理得到的用于提取环降时间的光谱数据[67]

feature increases with gas concentration. The continuous concentration measurement in Fig. 3(f) further demonstrates that the miniaturized hollow-waveguide gas cell can provide fast and stable dynamic response, with a response time of approximately 2.5 s in single-wavelength detection. These results highlight the potential of hollow waveguides for optical path compression, board-level integration, and portable gas detection. It should be noted that a longer hollow waveguide is not always preferable: although the absorption signal increases with length, propagation loss and background noise also increase. Therefore, the effective optical path length, coupling efficiency, transmission loss, and system volume must be comprehensively optimized.

Hollow-core fibers further improve the overlap between the optical field and gas sample. Hollow-core photonic bandgap fibers and anti-resonant hollow-core fibers can confine both light and gas within a micrometer-scale hollow core, enabling efficient interaction over long distances. In addition to direct absorption measurements, hollow-core fibers can be combined with photothermal phase detection, converting weak absorption signals into phase modulation signals. As shown in Fig. 3(g), a representative all-fiber photothermal interferometric sys-

tem[70] uses a 10 m long hollow-core photonic bandgap fiber as both the gas absorption region and the phase modulation region. The pump and probe beams strongly overlap with the target gas in the hollow core, and the photothermally induced phase change is read out through an interferometric structure. Fig. 3(h) shows the second-harmonic (2f) lock-in output obtained when the pump laser scans the absorption line of acetylene, with the signal amplitude increasing as the acetylene concentration rises from 50 ppm to 400 ppm. This system achieves a noise-equivalent concentration of approximately 2 ppb for acetylene and an equivalent absorption sensitivity of about 2.3×10^{-9} cm^{-1}, demonstrating the high-sensitivity detection capability of hollow-core fibers combined with photothermal phase readout. These studies show that the development of hollow-core fiber gas cells has progressed beyond path-length enhancement alone, and now involves coupled enhancement mechanisms based on photothermal effects, phase modulation, and interferometric readout.

On-chip waveguides represent a further step toward miniaturized and integrated gas interaction structures. Compared with discrete gas cells and hollow-core fibers, on-chip waveguides offer small footprint, batch manufacturability, and compatibility with integrated light sources, detectors, and electronic circuits, making them an important platform for chip-scale infrared gas sensing. However, because on-chip waveguides are physically short and the overlap between the evanescent field and gas molecules is limited, weak absorption detection usually requires higher interaction efficiency per unit length. Slow-light photonic crystal waveguides[71] provide an effective solution to this challenge. As shown in Fig. 3(i), a suspended silicon two-dimensional photonic crystal waveguide is integrated into the sensing arm of an on-chip Mach-Zehnder interferometer. The entire chip is approximately 4.5 mm long and 0.13 mm wide, in which a 1 mm long two-dimensional photonic crystal waveguide is used to enhance photothermal gas interaction, while a conventional strip waveguide serves as the reference arm. Through a dual slow-light mechanism, this structure simultaneously enhances pump absorption and probe phase modulation, enabling gas detection within a chip area of approximately 0.6 mm^2. Fig. 3(j) presents an Allan deviation analysis based on noise data, showing that the on-chip photothermal sensor achieves a C_2H_2 detection limit of approximately 12 ppm at an integration time of 200 s. This work indicates that on-chip gas sensing is shifting from merely reducing device size toward improving light-gas interaction efficiency per unit length through slow light, suspended structures, thermal management, and interferometric readout.

Overall, the development of gas interaction structures shows a clear trend toward spatial-scale compression. Discrete optical gas cells extend the effective optical path length through specular or diffuse reflection, making them suitable for high-sensitivity and multi-channel NDIR detection. Hollow waveguides compress meter-scale optical paths into flexible guiding channels, balancing portability and board-level integration. Hollow-core fibers enhance weak absorption detection through long-distance optical-field overlap and photothermal phase readout. On-chip photonic crystal waveguides use slow light and suspended structures to enhance interaction efficiency per unit length at the millimeter scale. In the future, the development of gas interaction structures will no longer simply pursue longer optical path lengths, but will seek an optimal balance among path length, loss, volume, response time, and integration level, in coordination with light sources, detectors, and spectral models.

4 Detectors: signal readout

Detectors are key components in infrared gas sensing systems for signal conversion, directly determining the noise level, response speed, operating temperature, spectral coverage, and cost of the system. According to their signal conversion mechanisms, infrared detectors can be broadly classified into photon detectors, thermal detectors, and photoacoustic/thermoelastic detectors, corresponding to "optical-to-electrical," "optical-to-thermal-to-electrical," and "absorbed-energy-to-thermal/acoustic/mechanical-vibration-to-electrical" readout pathways, respectively. These mechanisms offer different advantages in sensitivity, response speed, system complexity, and application scenarios, and together form the main development routes of the detection end in infrared gas sensing. Fig. 4 summarizes several representative detectors and signal readout mechanisms, illustrating the evolution of infrared gas sensing from semiconductor photodetection and array-based spectroscopic detection to on-chip spectral selection and thermoelastic readout.

Photon detectors generate electrical signals by exciting charge carriers in semiconductors with infrared photons, followed by the separation and collection of photogenerated carriers. They usually provide high response speed and high sensitivity, making them the most direct readout approach for high-performance infrared gas sensing. For mid-infrared detection, photon detectors generally require narrow-bandgap absorbing materials, while dark-current suppression and interface engineering are essential for improving room-temperature detection performance. A van der Waals complementary-barrier infrared detector based on BP/MoS_2[72] provides a representative example. As shown in Fig. 4(a), the device uses BP as the infrared absorption layer, forms an electron barrier through the Au/BP Schottky contact, and introduces a hole barrier using wide-bandgap MoS_2, thereby jointly suppressing thermally generated dark current in the narrow-bandgap material. The Arrhenius dark-current analysis in Fig. 4(b) further compares the dark-current behaviors of PN junction, unipolar-barrier, and complementary-barrier structures, demonstrating the role of complementary-barrier design in dark-current suppression. The device achieves a broadband room-temperature response from 290 to 3600 nm and a peak detectivity of 8.37×10^{-9} Jones under blackbody radiation testing. Fig. 4(c) shows its photoresponse under CH_4 concentrations

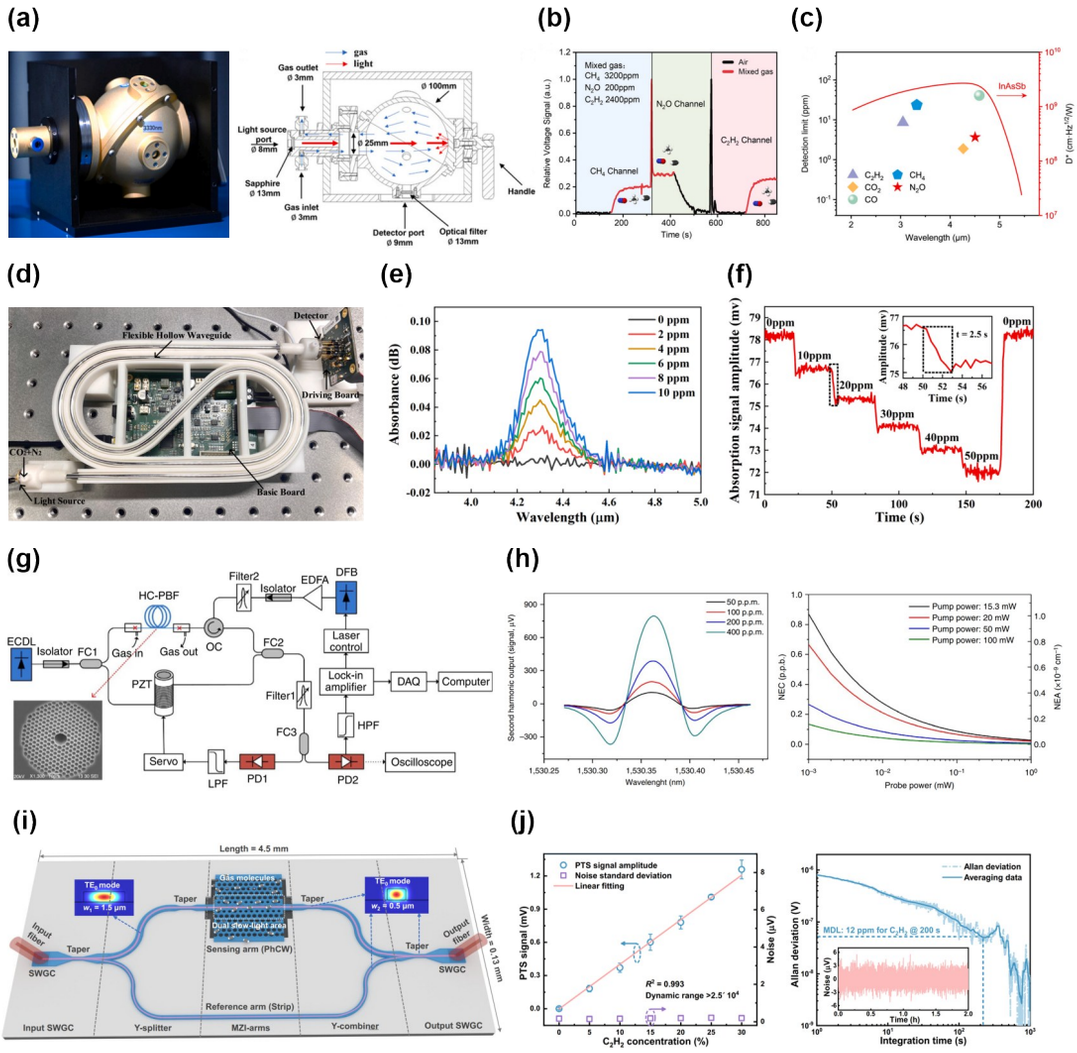

Fig. 3　Representative gas interaction structures for infrared gas sensing: (a)-(c) Rotating integrating sphere optical gas cell for compact multi-gas NDIR sensing, including the cell structure, mixed-gas sequential detection, and multi-gas detection limits[68]; (d)-(f) Board-level hollow waveguide gas cell for compact CO_2 sensing, including the experimental setup, concentration-dependent absorption spectra, and continuous concentration measurements[69]; (g), (h) Hollow-core photonic bandgap fiber for photothermal interferometric gas sensing, including the 10-m-long fiber-based experimental setup and second-harmonic acetylene signals at different concentrations[70]; (i), (j) On-chip photonic crystal waveguide for photothermal gas sensing, including the silicon-integrated Mach-Zehnder interferometer chip and Allan deviation analysis [71]

图 3　红外气体传感中的代表性气室:(a)-(c) 用于紧凑型多气体 NDIR 传感的旋转积分球光学气室,包括气室结构、混合气体顺序检测以及多气体检测限[68];(d)-(f) 用于紧凑型 CO2 传感的板级空心波导气室,包括实验装置、浓度相关吸收光谱以及连续浓度测量结果[69];(g), (h) 用于光热干涉式气体传感的空心光子带隙光纤,包括基于 10 m 长光纤的实验装置以及不同浓度下的乙炔二次谐波信号[70];(i), (j) 用于光热气体传感的片上光子晶体波导,包括硅基集成 Mach – Zehnder 干涉仪芯片以及 Allan 偏差分析[71]

ranging from 0 to 3%, with the methane absorption spectrum shown in the inset. Based on this device, NDIR methane detection with a detection limit of 23.9 ppm is achieved, indicating that two-dimensional-material photon detectors can not only serve infrared photodetection but also support compact gas sensing.

In advanced infrared spectroscopic systems, mature narrow-bandgap semiconductors such as mercury cadmium telluride (HgCdTe) remain important photon detector materials. Their bandgaps can be tuned by composition engineering to cover the near-infrared to mid- and far-infrared regions, and they offer high quantum efficiency and array-based readout capability. Therefore, they have long been used in high-resolution spectrometers and spaceborne remote sensing payloads. Taking the atmospheric carbon dioxide grating spectrometer on TanSat[73] as an example, as shown in Fig. 4(d), the payload contains three spectral channels, namely O_2 A-band (O_2A), weak CO_2 (WCO_2), and strong CO_2 (SCO_2) channels, operating at 0.758 – 0.778 μm, 1.594 – 1.624 μm, and 2.042 – 2.082 μm, respectively. The two CO_2 channels use HgCdTe focal plane arrays for high-resolution spectroscopic detection. The spectral resolving powers of the three channels reach approximately 19, 000, 12,

800, and 12,250, respectively, and long-term observational stability is ensured through in-orbit radiometric and wavelength calibration. Fig. 4(e) presents the global distribution of the signal-to-noise ratio for single observations in July 2018, showing that the O_2A, WCO_2, and SCO_2 bands all provide stable large-scale observations. Such systems demonstrate that, in spaceborne remote sensing, photon detectors are not isolated photoelectric conversion units, but are integrated with gratings, imaging optics, low-noise readout, temperature control, and radiometric calibration to form high-precision gas spectroscopic detection systems.

Thermal detectors convert absorbed infrared radiation into temperature changes and then convert the thermal signal into an electrical signal. Because they do not rely on photon energy directly exceeding a semiconductor bandgap, thermal detectors offer broadband spectral response, room-temperature operation, relatively low cost, and good array compatibility, and are widely used in compact NDIR gas sensing. Conventional thermal detectors usually operate together with external bandpass filters, whereas narrowband thermal detectors integrate the spectral selection function into the detector pixels themselves. As shown in Fig. 4(f), gold nanodisk antenna arrays[74] combined with metal-insulator-metal absorber structures can generate localized resonant absorption in selected mid-infrared bands and convert the absorbed energy into thermal signals. Fig. 4(g) further shows an NDIR architecture based on a metamaterial narrowband pyroelectric detector: broadband mid-infrared light passes through the gas cell and is then received by a multi-element narrowband pyroelectric detector array, in which different detector elements obtain different response peaks through nanoantenna design. A typical narrowband detector element near 5.52 μm exhibits a full width at half maximum of approximately 670 nm, a responsivity of about 90 V/W at a modulation frequency of 5 Hz, and a noise-equivalent power of 1.90×10^{-8} W $Hz^{-1/2}$. Fig. 4(h) shows that the measured narrowband responses of multiple metal – insulator – metal (MIM) absorber structures can be matched to the infrared absorption bands of eight gases, including H_2S, CH_4, CO_2, CO, NO, CH_2O, NO_2, and SO_2, enabling multi-gas NDIR detection. This strategy indicates that thermal detectors are evolving from broadband energy detection toward on-chip spectral selection and multi-channel functional detector arrays, providing a new detection-end solution for low-cost multi-gas NDIR sensing.

Photoacoustic and thermoelastic detectors read out weak signals through absorbed-energy conversion. Conventional photoacoustic spectroscopy detects acoustic waves generated by periodic gas absorption of modulated light, while quartz-enhanced photoacoustic spectroscopy further amplifies the acoustic response using a high-Q quartz tuning fork. Light-induced thermoelastic spectroscopy uses modulated light carrying gas absorption information to irradiate a quartz tuning fork, inducing light-driven thermoelastic vibration and generating an electrical signal through the piezoelectric effect. In this configuration, the tuning fork does not need to be directly placed in the target gas environment. As shown in Fig. 4(i), a recent CO-LITES (light-induced thermoelastic spectroscopy, LITES) system[75] combines an algorithm-optimized three-mirror multi-pass cell with a polydimethylsiloxane (PDMS)-modified low-frequency round-head quartz tuning fork. It achieves an effective optical path length of 25.8 m within a compact volume of 165.8 mL, corresponding to a path-length-to-volume ratio of 15.6 cm^{-2}. The system employs a 4.59 μm CO absorption line and a distributed-feedback quantum cascade laser (DFB-QCL) source with an optical power of approximately 145 mW. The low-frequency round-head quartz tuning fork has a resonance frequency of about 9.5 kHz, and after PDMS modification, the quartz tuning fork (QTF) signal is enhanced by approximately 10.59 times compared with that of a commercial quartz tuning fork. Fig. 4(j) shows the second-harmonic signals at different CO concentrations, demonstrating a clear concentration-dependent response to low-concentration CO. The Allan variance analysis in Fig. 4(k) further shows that the system achieves a detection limit of 23 ppt and a detection capability of 920.7 ppq at an integration time of 500 s. These studies indicate that photoacoustic/thermoelastic detection, through absorbed-energy conversion and mechanical resonance amplification, has outstanding potential for weak-absorption and ultra-trace gas detection.

Overall, the development of infrared detectors is expanding from single photoelectric conversion toward multi-mechanism energy-conversion readout. Photon detectors emphasize fast response, high sensitivity, and high-resolution spectroscopic readout, and can serve a wide range of systems from room-temperature NDIR sensors to spaceborne remote sensing instruments. Thermal detectors emphasize room-temperature operation, broadband response, and low cost, and are gaining on-chip spectral selection capability through metamaterial absorbers. Photoacoustic and thermoelastic detectors exploit absorbed-energy conversion and mechanical resonance amplification, showing high-sensitivity advantages for weak-absorption and ultra-trace detection. In the future, detector development will not only focus on the responsivity or detectivity of individual devices, but will also place greater emphasis on the coordinated optimization of detection mechanisms, spectral selection, noise suppression, array-based readout, and system integration.

5 Spectral models: information retrieval

As infrared gas sensing systems evolve toward miniaturization, low cost, and multi-component detection, spectral models are becoming increasingly important. Conventional high-resolution spectrometers can directly acquire complete absorption spectra, whereas compact sensing systems often provide only limited spectral bands, a small number of channels, or signals with low signal-to-noise ratios. Therefore, sensing performance depends not only on the light source, gas interaction structure, and detector, but also on how spectral sampling windows are selected, how component information

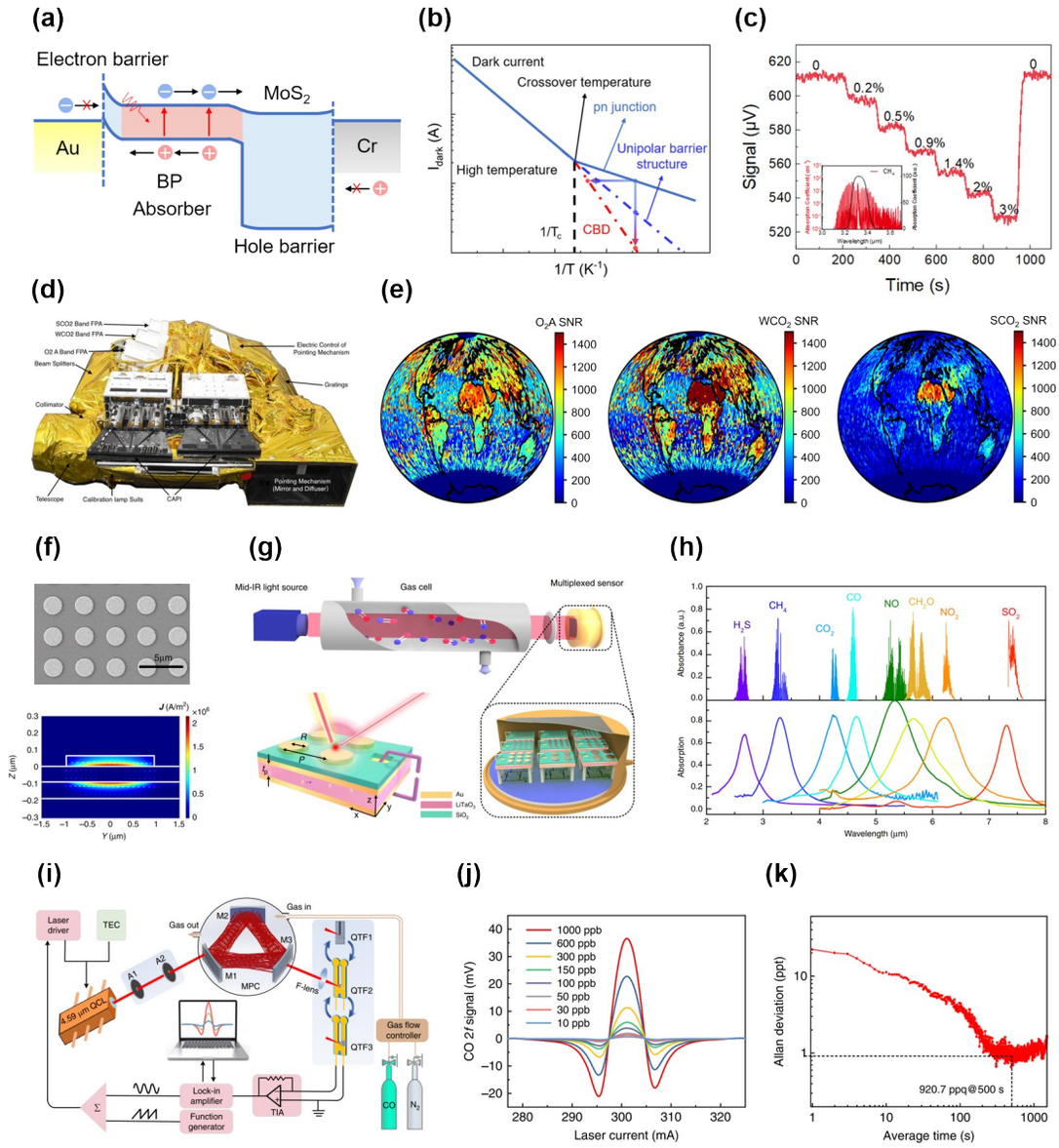

Fig. 4　Representative infrared detectors and signal readout mechanisms for gas sensing: (a)-(c) Two-dimensional-material-based van der Waals complementary barrier infrared detector for room-temperature NDIR methane sensing, including the device band diagram, dark-current Arrhenius analysis, and methane photoresponse from 0 to 3%[72]; (d), (e) HgCdTe focal plane array detectors for satellite-based atmospheric CO_2 spectroscopy, including the in-flight atmospheric carbon dioxide grating spectrometer and global single-sounding SNR maps for the O_2A, WCO_2, and SCO_2 bands[73]; (f)-(h) Metamaterial-integrated narrowband pyroelectric detectors for multi-gas NDIR sensing, including the gold nanodisk antenna array, detector-integrated NDIR architecture, and spectral matching with eight gas absorption bands[74]; (i)-(k) CO light-induced thermoelastic spectroscopy based on an optimized multi-pass cell and a PDMS-modified quartz tuning fork, including the sensor schematic, concentration-dependent 2f signals, and Allan variance analysis[75]

图 4　气体传感中的代表性探测器:(a)-(c) 基于二维材料的范德华互补势垒红外探测器,用于室温 NDIR 甲烷传感,包括器件能带图、暗电流 Arrhenius 分析以及 0-3% 甲烷光响应[72];(d), (e) 用于卫星大气 CO2 光谱探测的 HgCdTe 焦平面阵列探测器,包括在轨大气二氧化碳光栅光谱仪以及 O2A、WCO2 和 SCO2 波段的全球单次观测 SNR 分布图[73];(f)-(h) 用于多气体 NDIR 传感的超材料集成窄带热释电探测器,包括金纳米圆盘天线阵列、探测器集成式 NDIR 架构以及与八种气体吸收带的光谱匹配[74];(i)-(k) 基于优化多通池和 PDMS 修饰石英音叉的 CO 光诱导热弹光谱,包括传感器示意图、浓度相关 2f 信号以及 Allan 方差分析[75]

is extracted from overlapping spectra, and how robust retrieval is achieved under complex background conditions. Fig. 5 summarizes three representative types of spectral models, including sampling optimization models, linear retrieval models, and nonlinear intelligent retrieval models. These three categories correspond, respectively, to the questions of how to acquire effective spectral information, how to separate overlapping component contributions, and how to achieve robust identification and prediction under complex conditions.

For low-resolution or few-channel NDIR systems, spectral modeling first appears as the optimization of sam-

pling strategies. Conventional filter selection usually emphasizes whether the center wavelength is aligned with the absorption peak of the target gas. However, practical sensing performance is jointly affected by the filter bandwidth, source spectrum, detector response, and noise level. An overly narrow bandwidth may exclude a large amount of useful absorption light and reduce sensitivity, whereas an overly broad bandwidth may introduce more non-absorbing background light, increasing noise and degrading the signal-to-noise ratio. Therefore, the optimal sampling window does not necessarily correspond to the strongest single absorption peak, but should instead balance the integrated absorption signal and the noise contribution. As shown in Fig. 5(a)-(c), an optical bandwidth matching method[76] is demonstrated using CO detection as an example. Five filters with different center wavelengths and bandwidths are compared, and the detection limits under different spectral bandwidths are tested. By establishing the relationship among detection limit, sensitivity, and noise, this method calculates the performance distribution corresponding to different center wavelengths and bandwidths under shot-noise-dominated conditions. The experimental results agree well with the theoretical predictions, with the optimal filter located near 4665 nm and 240 nm full width at half maximum (FWHM), corresponding to a CO detection limit of 11.34 ppm. These results show that sampling-window design itself can serve as an effective system optimization strategy for guiding filter selection, channel design, and performance prediction in NDIR sensors.

When continuous or multi-channel spectral information is available, the role of spectral models further shifts toward multi-component concentration retrieval. For complex gas mixtures, the absorption spectra of different molecules often strongly overlap, and a single wavelength or channel is usually insufficient to provide adequate selectivity. Partial least-squares regression[77] is a representative linear multivariate retrieval method. It reduces the dimensionality of high-dimensional spectral data by constructing latent variables and maximizes the covariance between the spectral matrix and the concentration matrix, thereby alleviating the instability caused by collinearity among spectral variables and overlapping absorption features. As shown in Fig. 5(d), an experimental system based on a mid-infrared supercontinuum source uses an 11.6 cm absorption cell and a spectral analyzer with a resolution of 0.5 cm^{-1} to reconstruct the broadband absorption spectra of CH_4, C_2H_6, and C_3H_8 in the 2850 – 3175 cm^{-1} region. For natural-gas-like mixtures, the C-H stretching absorption bands of these three alkanes strongly overlap, and their concentration ratios are highly unbalanced. Fig. 5(e), (f) compare the spectral reconstruction performance of multiple linear regression (MLR) and partial least-squares regression (PLSR) for mixed-gas spectra, showing that PLSR can more effectively separate the spectral contributions of different components. In three-component mixture analysis, MLR achieves average prediction accuracies of 91%, 68%, and 75% for CH_4, C_2H_6, and C_3H_8, respectively, whereas PLSR improves these values to 98%, 93%, and 94%. These results indicate that linear latent-variable models can effectively enhance the multi-component analytical capability of broadband infrared sensing while maintaining relatively low computational complexity.

In more complex application scenarios, infrared spectral signals can also be affected by low signal-to-noise ratios, variations in background radiation, nonuniform instrument response, and nonlinear radiative transfer. Traditional linear models are often unable to fully describe the complex mapping between measured signals and gas species or concentrations. Machine learning and deep learning methods therefore provide more flexible tools for nonlinear modeling. The Cross-talk Transformer[78] developed for uncooled snapshot infrared spectroscopic imaging systems is a representative example of this direction. As shown in Fig. 5(g), the uncooled snapshot infrared spectral imager (USIRS) system uses multi-channel infrared spectroscopic imaging over the 7-14 μm range to realize long-distance gas identification and concentration prediction. This method first establishes a radiative transfer model that includes background radiation, gas radiation, atmospheric transmission, optical-system transmittance, detector response, and noise to generate large-scale simulated data. Then, as shown in Fig. 5(h), a convolutional neural network (CNN) is used to extract shallow features from low-SNR signals and the gas spectral library, while a Transformer attention mechanism learns the deep correlation between the measured signal and the standard spectral library. Finally, two multilayer perceptron (MLP) branches are used for classification and regression, outputting the gas species and concentration, respectively. Fig. 5(i) shows the model training process and concentration prediction results. On experimental data, this method achieves a recognition accuracy of 98.63% for 11 gases and a root-mean-square error (RMSE) of 0.51 kppm over a concentration range up to 30,000 ppm, outperforming comparison methods such as CNN, MLP, and conventional Transformer models. This type of work indicates that nonlinear intelligent retrieval is not simply replacing physical models, but is moving toward the integration of physical radiative transfer, spectral priors, and data-driven networks.

Despite these advances, the physical interpretability and generalizability of data-driven spectral models remain major barriers to practical deployment. Most current models are trained using simulated spectra or closed datasets covering predefined gas species, concentration ranges, environmental conditions, and instrument responses. Their performance may therefore degrade for unseen gas mixtures, unexpected interferents, temperature- and pressure-induced spectral shifts, detector aging, or calibration drift. Moreover, black-box predictions make it difficult to determine whether a model has learned molecular absorption features or dataset-specific correlations. Future work should emphasize external validation across instruments and operating conditions, uncertainty quantification, domain adaptation, transfer

learning, and continual calibration. Physics-informed and hybrid models that embed the Beer-Lambert law, radiative-transfer relationships, spectral databases, or instrument-response functions into network architectures or loss functions provide a promising route to improving interpretability, data efficiency, and out-of-distribution robustness.

Overall, the development of spectral models reflects a progression from sampling design to information interpretation. Sampling optimization models address how to acquire the most effective spectral information under limited hardware conditions. Linear retrieval models address how to separate component contributions from multi-channel or continuous spectra. Nonlinear intelligent models target robust identification and concentration prediction under complex backgrounds, low-SNR conditions, and nonlinear system responses. In the future, spectral models will no longer serve merely as back-end data processing tools, but will become an essential part of infrared gas sensing system design.

6 Discussion and outlook

The development of infrared gas sensing is not a linear process in which one technical route simply replaces another. Instead, it represents the parallel evolution of multiple approaches driven by different application requirements. The central issue has always been how to

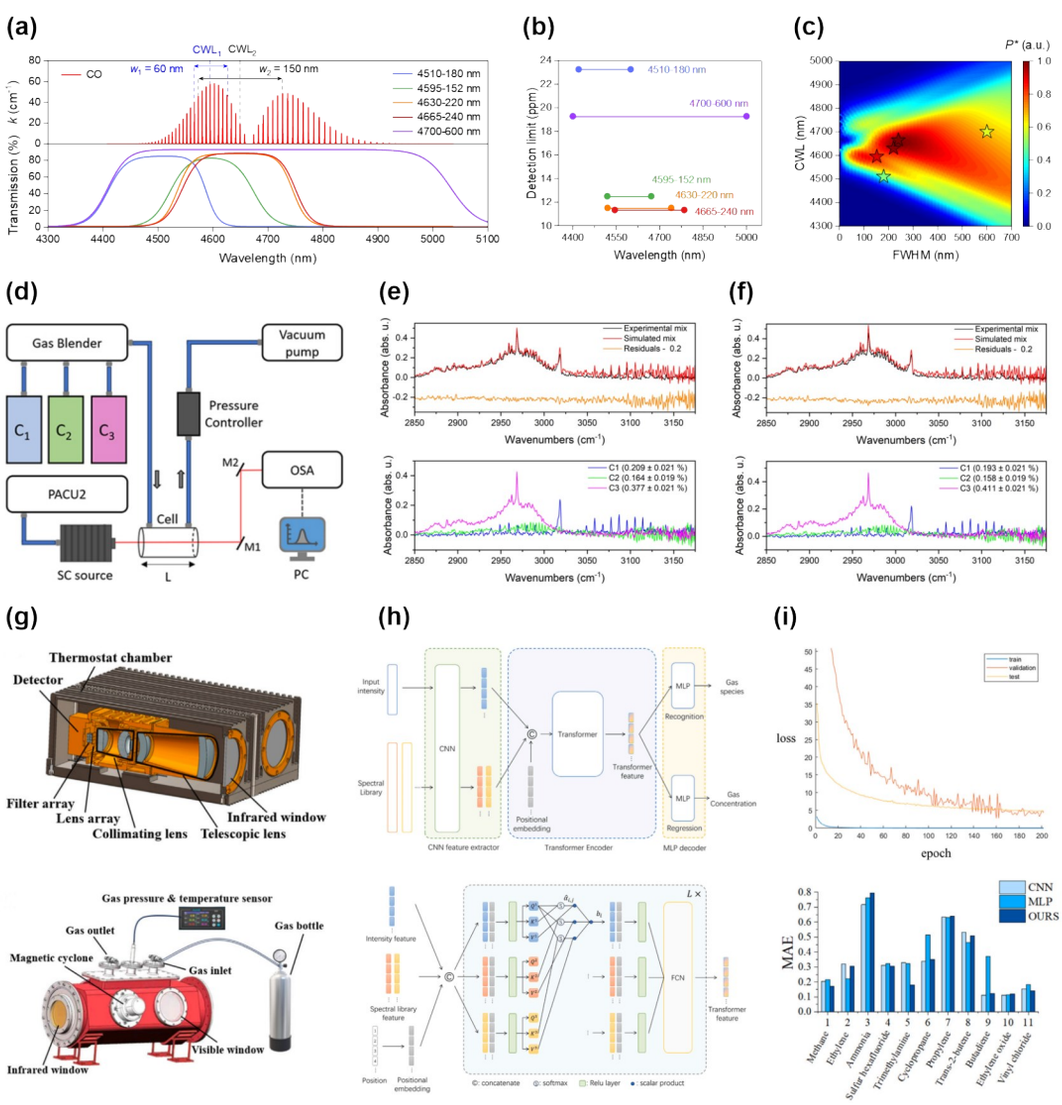

Fig. 5 Representative spectral models for infrared gas sensing: (a)-(c) Sampling optimization model based on optical bandwidth matching for CO detection, including filter selection, bandwidth-dependent detection-limit evaluation, and theoretical performance mapping[76]; (d)-(f) Linear retrieval models for multi-gas analysis, including broadband absorption spectra of CH_4, C_2H_6, and C_3H_8, and spectral reconstruction based on MLR and PLSR[77]; (g)-(i) Nonlinear intelligent retrieval model based on the Cross-talk Transformer for gas recognition and concentration prediction, including the USIRS, network architecture, and prediction results[78]

图 5 红外气体传感中的代表性光谱模型:(a)-(c) 基于光带宽匹配的采样优化模型,用于 CO 检测,包括滤光片选择、带宽相关的检测限评估以及理论性能分布图[76];(d)-(f) 用于多气体分析的线性反演模型,包括 CH4、C2H6 和 C3H8 的宽带吸收光谱,以及基于 MLR 和 PLSR 的光谱重构[77];(g)-(i) 基于 Cross-talk Transformer 的非线性智能反演模型,用于气体识别和浓度预测,包括 USIRS 系统、网络结构以及预测结果[78]

balance sensitivity, selectivity, system scale, optical path length, response speed, power consumption, cost, and environmental adaptability. High-sensitivity detection usually requires stronger molecular absorption, longer effective optical path lengths, lower noise, and more refined spectral analysis. In contrast, portable, field-deployable, and on-chip applications place greater emphasis on compact structure, low power consumption, low cost, and system integration. Therefore, infrared gas sensing technologies should not be evaluated using a single metric alone, but rather through a comprehensive assessment that considers the target gas, operating spectral region, detection limit, optical path length, and application scenario.

Fig. 6(a) presents the performance distribution of representative infrared gas sensing studies in terms of detection limit, operating wavelength, and effective optical path length (see details in Table 1). It can be seen that both near-infrared and mid-infrared regions have supported a variety of mature detection schemes, among which the mid-infrared region plays an important role in trace gas detection and complex gas analysis because it corresponds to the fundamental absorption bands of many gas molecules. Differences in detection limits among different technologies arise not only from absorption strength, but also from light-source brightness, gas interaction length, detector noise, and signal processing methods. Long-path multi-pass cells, cavity-enhanced structures, hollow-core fibers, and photoacoustic/thermoelastic readout methods can significantly enhance weak absorption signals and therefore show outstanding performance in achieving low detection limits. In contrast, NDIR sensors, waveguide sensors, on-chip photonic structures, and multivariate spectral models offer unique advantages in system compactness, low power consumption, multichannel detection, and application adaptability. The optical path length represented by the scatter size further indicates the intrinsic relationship between detection sensitivity and system scale: longer path lengths help enhance absorption signals, whereas shorter path lengths and smaller volumes require stronger absorption bands, lower-noise detection, optical-field-enhancement structures, or spectral models to improve information utilization efficiency per unit system scale.

Fig. 6(b) further summarizes the application landscape of infrared gas sensing from the perspective of spatial scale. Infrared gas sensing now covers multiple levels, ranging from global atmospheric remote sensing, regional gas monitoring, open-path and in situ detection, to portable sensors and on-chip gas sensing chips. The technical emphasis varies across these scales. Global and regional monitoring require broad spectral coverage, radiometric calibration, long-term stability, and robust retrieval models. Industrial field and in situ detection focus more on sensitivity, response speed, anti-interference capability, and system reliability. Miniaturized and on-chip systems place greater emphasis on low power consumption, low cost, batch manufacturability, and optoelectronic integration. These characteristics show that infrared gas sensing is not a fixed-form detection technique, but rather a flexible technological platform that can be configured according to monitoring distance, concentration range, target gas species, and system constraints.

To complement the point-by-point comparison in Fig. 6(a), Fig. 6(c) provides a normalized semi-quantitative benchmark of nine representative technical routes. The methods are organized, from left to right, into direct absorption spectroscopy, cavity-enhanced spectroscopy, and indirect absorption spectroscopy. Each method is scored from 1 to 5 in six dimensions: sensitivity, selectivity, multi-gas capability, commercial maturity, practicality, and miniaturization. The scores synthesize the representative literature summarized in this review together with typical system complexity and component availability, and are intended to reveal relative trade-offs rather than serve as absolute performance specifications. In this assessment, practicality incorporates typical power demand, response time, alignment and calibration requirements, and maintenance burden; commercial maturity reflects component availability, manufacturing repeatability, and cost; and miniaturization reflects the attainable system volume and integration potential.

The comparison reveals distinct technology-dependent trade-offs. Among direct absorption methods, NDIR offers the strongest combination of low cost, compactness, and deployment maturity, but its moderate sensitivity and selectivity limit trace analysis; TDLAS improves sensitivity and selectivity while retaining relatively fast response, but requires a tunable laser, wavelength control, and more complex calibration; Fourier transform infrared spectroscopy (FTIR) provides the best multi-gas capability but generally entails a larger optical platform, higher power consumption, and greater cost. Cavity-enhanced methods provide the highest sensitivity and selectivity through kilometer-equivalent effective path lengths, but the stringent requirements for high-reflectivity mirrors, mode matching, frequency locking, and cavity cleanliness increase volume, cost, and maintenance complexity. Off-axis integrated cavity output spectroscopy (OA-ICOS) relaxes alignment and locking requirements relative to cavity ring-down spectroscopy (CRDS) and therefore achieves a more favorable practicality score. Among indirect methods, photoacoustic spectroscopy (PAS) provides a comparatively balanced route with high sensitivity and moderate system complexity, whereas photothermal spectroscopy (PTS) and LITES avoid conventional photodetectors and offer strong miniaturization potential. Their broader adoption, however, is still constrained by dependence on high-power modulated sources, resonance stability, specialized transducers, and less mature calibration and packaging processes. Consequently, no single approach is universally optimal: technology selection should be based on the required concentration range, number of analytes, allowable response time, power and volume budgets, and total system cost.

Translating laboratory performance into field opera-

tion introduces a different set of constraints. Temperature and humidity variations can change absorption-line strengths, gas density, refractive index, optical alignment, and transducer resonance; contamination and optical aging can reduce source power or cavity and waveguide transmission; and detector and electronic drift can gradually invalidate calibration. These effects require reference channels, temperature-pressure-humidity compensation, automated baseline correction, periodic recalibration, and long-duration validation under realistic gas matrices. Technology readiness also differs markedly. NDIR, TDLAS, FTIR, and several cavity-enhanced analyzers have mature commercial implementations, although high-end laser and cavity systems remain limited by cost and maintenance. PAS has progressed to field and commercial instruments, whereas many quartz-enhanced photoacoustic spectroscopy (QEPAS), PTS, LITES, metasurface, and on-chip waveguide demonstrations remain at laboratory or prototype level. For these emerging approaches, manufacturing yield, device-to-device variation, hermetic and contamination-resistant packaging, fiber or free-space coupling tolerance, and reproducible mass calibration are as important as the minimum detection limit. Technology-readiness claims should therefore be application specific and supported by environmental, lifetime, and batch-level tests rather than inferred from short-term laboratory sensitivity alone.

From the perspective of technological evolution, the progress of infrared gas sensing is mainly reflected in four aspects. The development of infrared light sources provides the basis for gas analysis across different spectral regions, resolutions, and system complexities. From broadband thermal emitters and tunable semiconductor sources to lasers and frequency combs, light sources are providing increasingly rich and controllable spectral information. The development of gas interaction structures promotes the balance between optical path enhancement and spatial compression, with free-space gas cells, hollow waveguides, hollow-core fibers, and on-chip waveguides addressing different sensing scales and integration requirements. The development of infrared detectors has expanded signal readout pathways, with photon, thermal, and photoacoustic/thermoelastic detection mechanisms offering distinct advantages in high sensitivity, broadband response, room-temperature operation, and weak-absorption detection. The development of spectral models further improves the utilization efficiency of limited spectral information, with sampling optimization, multivariate regression, and machine learning providing new tools for low-resolution, few-channel, multi-component, and complex-background gas analysis.

Several emerging frontiers may further reshape this landscape. First, metasurface-based platforms can integrate wavelength-selective absorption, filtering, beam shaping, and detector functions within subwavelength structures, enabling compact multi-channel and computational gas sensors. Their main challenges are resonance drift, fabrication tolerance, limited interaction length, and scalable packaging. Second, quantum-enhanced spectroscopy uses nonclassical states and optical correlations to reduce measurement noise below the coherent-state shot-noise limit. Quantum correlation-enhanced dual-comb spectroscopy has demonstrated a 2 dB signal-to-noise improvement beyond the shot-noise limit and comb-line-resolved spectroscopy near 3 μm[79], although optical loss, detector efficiency, source complexity, and environmental stability currently restrict practical gas-sensing deployment. Third, mid-infrared photonic integrated circuits are evolving from isolated waveguide sensors toward co-integrated sources, routing structures, interaction regions, filters, and detectors. Recent multifunctional lithium-niobate platforms and co-packaged QCL modules illustrate a route toward integrated spectroscopic systems[80]. Achieving true monolithic integration will require heterogeneous material integration, low-loss broadband coupling, thermal isolation, gas-accessible packaging, and wafer-scale calibration.

Therefore, the future development of infrared gas sensing should not focus on the isolated improvement of a single metric, but should instead establish a more appropriate performance balance for specific applications. For trace detection and high-precision analysis, strong absorption bands, high-brightness light sources, long effective optical paths, and low-noise detectors remain essential. For multi-component detection and complex-background analysis, broadband coverage, multi-channel sampling, and intelligent spectral interpretation will play increasingly important roles. For field deployment and portable applications, system stability, cost, power consumption, and response speed are equally critical. For on-chip gas sensing, an important frontier is how to enhance light-gas interaction within a limited footprint while realizing the coordinated integration of light sources, waveguides, detectors, and readout circuits.

Three actionable research gaps deserve particular attention. First, the fundamental sensitivity limit of chip-scale sensing must be established by separating molecular shot noise, optical loss, source relative-intensity noise, detector noise, thermal fluctuations, and adsorption-related drift. Breakthroughs are likely to require slow-light or resonant field enhancement without excessive loss, stronger evanescent-field overlap, differential or self-referenced architectures, and low-noise on-chip photothermal or photoacoustic transduction. Second, fair cross-technology benchmarking requires standardized reporting of detection limit together with averaging time, optical power, path length, gas-cell volume, pressure, temperature, humidity, flow rate, response and recovery times, calibration interval, and long-term drift. Reporting normalized absorption sensitivity and energy- or volume-normalized performance alongside application-level metrics would reduce misleading comparisons based on detection limit alone. Third, monolithic mid-infrared integration remains limited by incompatible material platforms for sources, low-loss waveguides, modulators, and detectors; thermal cross-talk from electrically driven sources; coupling and packaging losses; and the need to expose the sensing region to gas while protecting active

devices. Addressing these gaps will require co-design across materials, photonics, electronics, microfluidics, packaging, and retrieval algorithms, together with wafer-level yield and reliability studies.

Overall, infrared gas sensing has evolved from conventional absorption spectroscopy into an integrated technological system involving light sources, gas interaction structures, detectors, and spectral models. Different technical routes have distinct positions in terms of sensitivity, spectral region, optical path length, volume, and application scale, together forming the current technological landscape of infrared gas sensing. By combining performance distribution with spatial scale, the applicable scenarios and development potential of different technologies can be more clearly understood. In the future, with continued advances in infrared optoelectronic devices, micro- and nanophotonic structures, high-performance detectors, and intelligent retrieval methods, infrared gas sensing is expected to further expand its application boundaries toward high sensitivity, multi-component analysis, miniaturization, intelligence, and integration.

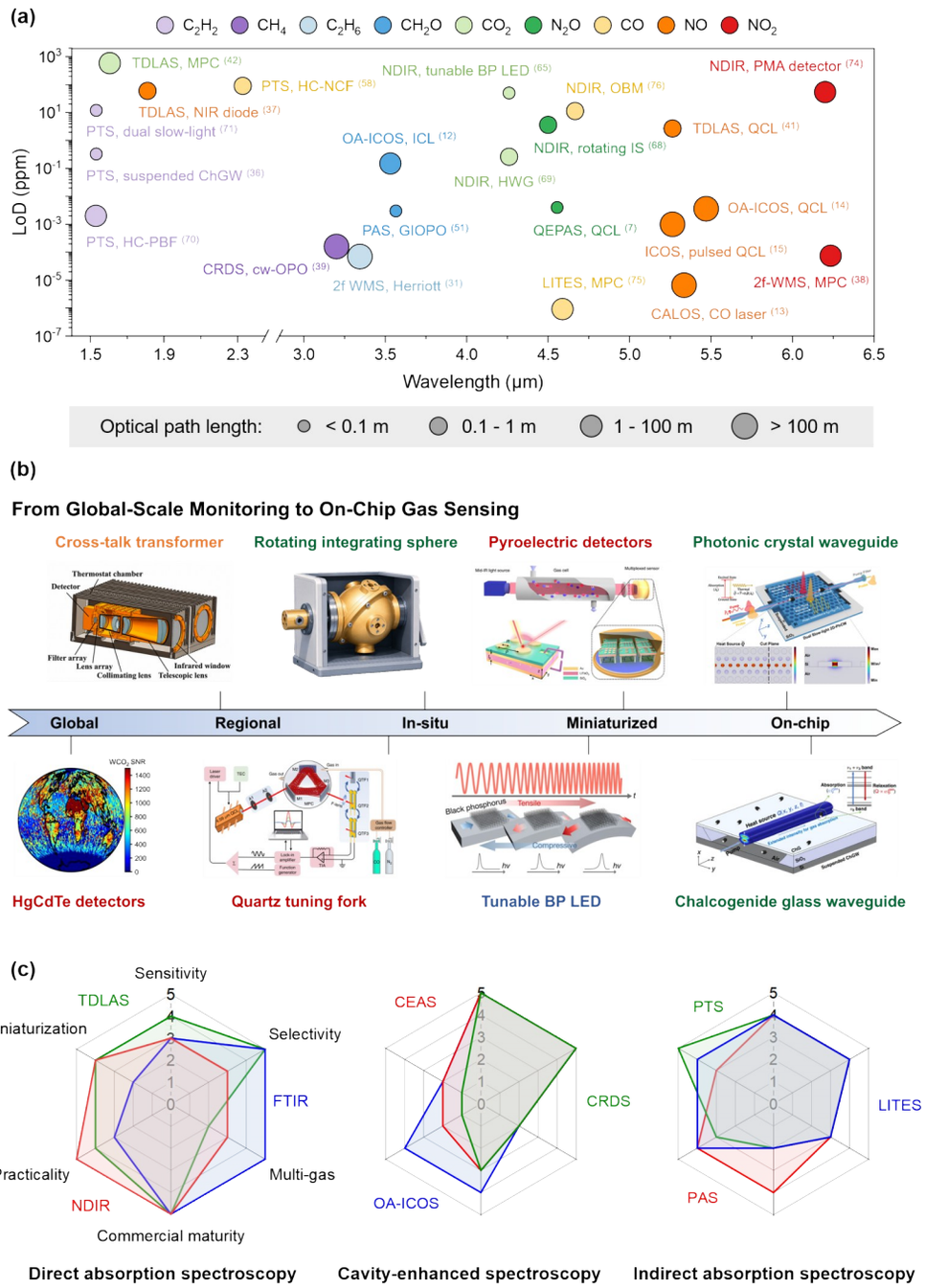

Fig. 6　Summary of infrared gas sensing technologies from performance and spatial-scale perspectives: (a) Performance landscape of representative studies, showing the relationship among operating wavelength, detection limit, target gas species, and optical path length. The color of each marker denotes the detected gas species, the marker size represents the optical path length, and the text label indicates the main sensing technique (see Table 1 for corresponding references); (b) Spatial-scale distribution of representative infrared gas sensing technologies, illustrating their applications from global atmospheric monitoring and regional remote sensing to in-situ detection, miniaturized sensing systems, and on-chip gas sensing[73,78,75,68,65,74,71,36]; (c) Normalized semi-quantitative comparison of representative technologies across sensitivity, selectivity, multi-gas capability, commercial maturity, practicality, and miniaturization. From left to right, the radar charts compare direct absorption spectroscopy (NDIR, TDLAS, and FTIR), cavity-enhanced spectroscopy (CEAS, CRDS, and OA-ICOS), and indirect absorption spectroscopy (PAS, PTS, and LITES), respectively. Each metric is rated from 1 to 5, with a higher score indicating stronger relative performance

图 6　从性能和空间尺度角度对红外气体传感技术进行总结:(a) 代表性研究的性能分布图,展示了工作波长、检测限、目标气体种类和光程长度之间的关系。其中,散点颜色表示检测气体种类,散点大小表示光程长度,文字标注表示主要传感技术(参考文献详见表 1);(b) 代表性红外气体传感技术的空间尺度分布,展示了其从全球大气监测、区域遥感到原位检测、小型化传感系统以及片上气体传感等不同应用层级[73,78,75,68,65,74,71,36];(c) 代表性技术在灵敏度、选择性、多气体检测能力、商业成熟度、实用性和小型化程度方面的归一化半定量比较。从左到右,三张雷达图依次比较直接吸收光谱(NDIR、TDLAS 和 FTIR)、腔增强光谱(CEAS、CRDS 和 OA-ICOS)以及间接吸收光谱(PAS、PTS 和 LITES)。各项指标采用 1 – 5 分制,分值越高表示相应的相对性能越优

Table 1 | Representative infrared gas sensing technologies and their key performance metrics
表 1 | 代表性红外气体传感技术及其关键性能指标

Ref.	Gas	λ (μm)	L (m)	LoD (ppm)	Method
[70]	C_2H_2	1.530	1.0×10^{1}	2.0×10^{-3}	PTS, HC-PBF
[71]	C_2H_2	1.532	1.0×10^{-3}	1.2×10^{1}	PTS, dual slow-light
[36]	C_2H_2	1.532	1.2×10^{-2}	3.3×10^{-1}	PTS, suspended ChGW
[42]	CO_2	1.606	1.5×10^{1}	5.9×10^{2}	TDLAS, MPC
[37]	NO	1.810	5.0×10^{-1}	6.0×10^{1}	TDLAS, NIR diode
[58]	CO	2.327	8.5×10^{-1}	9.0×10^{1}	PTS, HC-NCF
[39]	CH_4	3.200	3.5×10^{3}	1.6×10^{-4}	CRDS, cw-OPO
[31]	C_2H_6	3.344	2.0×10^{2}	7.0×10^{-5}	2f WMS, Herriott
[12]	CH_2O	3.531	2.0×10^{1}	1.5×10^{-1}	OA-ICOS, ICL
[51]	CH_2O	3.565	4.0×10^{-2}	3.0×10^{-3}	PAS, GIOPO
[65]	CO_2	4.260	5.1×10^{-2}	5.0×10^{1}	NDIR, tunable BP LED
[69]	CO_2	4.260	1.0×10^{0}	2.6×10^{-1}	NDIR, HWG
[68]	N_2O	4.500	6.6×10^{-1}	3.6×10^{0}	NDIR, rotating IS
[7]	N_2O	4.555	5.3×10^{-3}	4.0×10^{-3}	QEPAS, QCL
[75]	CO	4.588	2.6×10^{1}	9.2×10^{-7}	LITES, MPC
[76]	CO	4.665	8.0×10^{-1}	1.1×10^{1}	NDIR, OBM
[15]	NO	5.263	1.5×10^{3}	1.0×10^{-3}	ICOS, pulsed QCL
[41]	NO	5.263	2.1×10^{-1}	2.7×10^{0}	TDLAS, QCL
[13]	NO	5.334	2.7×10^{3}	6.6×10^{-6}	CALOS, CO laser
[14]	NO	5.470	5.0×10^{3}	3.6×10^{-3}	OA-ICOS, QCL
[74]	NO_2	6.200	5.0×10^{0}	5.4×10^{1}	NDIR, PMA detector
[38]	NO_2	6.234	4.0×10^{1}	7.5×10^{-5}	2f-WMS, MPC

Abbreviations: LoD, limit of detection; PTS, photothermal spectroscopy; HC-PBF, hollow-core photonic bandgap fiber; ChGW, chalcogenide glass waveguide; TDLAS, tunable diode laser absorption spectroscopy; MPC, multi-pass cell; NIR, near-infrared; HC-NCF, hollow-core negative-curvature fiber; CRDS, cavity ring-down spectroscopy; cw-OPO, continuous-wave optical parametric oscillator; WMS, wavelength modulation spectroscopy; OA-ICOS, off-axis integrated cavity output spectroscopy; ICOS, integrated cavity output spectroscopy; ICL, interband cascade laser; PAS, photoacoustic spectroscopy; GIOPO, grating-tuned intracavity optical parametric oscillator; NDIR, non-dispersive infrared; BP, black phosphorus; LED, light-emitting diode; HWG, hollow waveguide; IS, integrating sphere; QEPAS, quartz-enhanced photoacoustic spectroscopy; QCL, quantum cascade laser; LITES, light-induced thermoelastic spectroscopy; OBM, optical bandwidth matching; CALOS, cavity leak-out spectroscopy; PMA, pyroelectric metamaterial absorber.

References

[1] Hodgkinson J, Tatam R P. Optical gas sensing: a review[J]. Measurement Science and Technology, 2013, 24(1): 012004.

[2] Zheng C, Pi M, Song F, et al. Recent progress in infrared absorption spectroscopy for gas sensing with discrete optics, hollow-core fibers and on-chip waveguides [J]. Journal of Lightwave Technology, 2023, 41(13): 4079-4096.

[3] Da Silveira Petruci J F, Da Silva Sousa D, Mizaikoff B. Advanced mid-infrared sensors for molecular analysis[J]. Analytical Chemistry, 2025, 97(13): 6871-6890.

[4] Soref R. Mid-infrared photonics in silicon and germanium[J]. Nature Photonics, 2010, 4(8): 495-497.

[5] Barron-Jimenez R, Caton J A, Anderson T N, et al. Application of a difference-frequency-mixing based diode-laser sensor for carbon monoxide detection in the 4.4 – 4.8 μm spectral region [J]. Applied Physics B, 2006, 85(2-3): 185-197.

[6] Kormann R, Königstedt R, Parchatka U, et al. QUALITAS: A mid-infrared spectrometer for sensitive trace gas measurements based on quantum cascade lasers in CW operation[J]. Review of Scientific Instruments, 2005, 76(7): 075102.

[7] Kosterev A A, Bakhirkin Y A, Tittel F K. Ultrasensitive gas detection by quartz-enhanced photoacoustic spectroscopy in the fundamental molecular absorption bands region[J]. Applied Physics B, 2005, 80(1): 133-138.

[8] Huszár H, Pogány A, Bozóki Z, et al. Ammonia monitoring at ppb level using photoacoustic spectroscopy for environmental application[J]. Sensors and Actuators B: Chemical, 2008, 134(2): 1027-1033.

[9] Moeskops B W M, Cristescu S M, Harren F J M. Sub-part-per-billion monitoring of nitric oxide by use of wavelength modulation spectroscopy in combination with a thermoelectrically cooled, continuous-wave quantum cascade laser [J]. Optics Letters, 2006, 31(6): 823.

[10] Von Basum G, Halmer D, Hering P, et al. Parts per trillion sensitivity for ethane in air with an optical parametric oscillator cavity leak-out spectrometer[J]. Optics Letters, 2004, 29(8): 797.

[11] Patimisco P, Sampaolo A, Dong L, et al. Recent advances in quartz enhanced photoacoustic sensing[J]. Applied Physics Reviews, 2018, 5(1): 011106.

[12] Miller J H, Bakhirkin Y A, Ajtai T, et al. Detection of formaldehyde using off-axis integrated cavity output spectroscopy with an interband cascade laser[J]. Applied Physics B, 2006, 85(2-3): 391-396.

[13] Heinrich K, Fritsch T, Hering P, et al. Infrared laser-spectroscopic analysis of ^{14}NO and ^{15}NO in human breath[J]. Applied Physics B, 2009, 95(2): 281-286.

[14] McCurdy M R, Bakhirkin Y A, Tittel F K. Quantum cascade laser-based integrated cavity output spectroscopy of exhaled nitric oxide[J]. Applied Physics B, 2006, 85(2-3): 445-452.

[15] Silva M L, Sonnenfroh D M, Rosen D I, et al. Integrated cavity output spectroscopy measurements of NO levels in breath with a pulsed room-temperature QCL[J]. Applied Physics B, 2005, 81(5): 705-710.

[16] Wysocki G, Bakhirkin Y, So S, et al. Dual interband cascade laser based trace-gas sensor for environmental monitoring[J]. Applied Optics, 2007, 46(33): 8202.

[17] Hamilton D J, Orr-Ewing A J. A quantum cascade laser-based optical feedback cavity-enhanced absorption spectrometer for the simultaneous measurement of CH_4 and N_2O in air [J]. Applied Physics B, 2011, 102(4): 879-890.

[18] McManus J B, Shorter J H, Nelson D D, et al. Pulsed quantum cascade laser instrument with compact design for rapid, high sensitivity measurements of trace gases in air[J]. Applied Physics B, 2008, 92(3): 387.

[19] Yi Zi-Yuan, Tang Bo-Cheng, Xiong Zi-Ying, et al. Broadband and high-sensitivity cavity-enhanced dual-comb spectroscopy for gas absorption measurements[J]. Journal of Infrared and Millimeter Waves, 2026, 45(5):
(易子渊,汤博诚,熊子颖,等. 宽带、高灵敏腔增强双光梳气体吸收光谱测量技术研究[J]. 红外与毫米波学报), 2026, 45(5):.

[20] Wang W, Zhang T, Zhang Q, et al. Photoacoustic spectroscopy sensor based on a dual-resonance photoacoustic cell for simultaneous detection of two-component gases[J]. Infrared Physics &

Technology, 2025, 150: 106047.
[21] Crosson E R. A cavity ring-down analyzer for measuring atmospheric levels of methane, carbon dioxide, and water vapor[J]. Applied Physics B, 2008, 92(3): 403-408.
[22] Rawlins W T, Hensley J M, Sonnenfroh D M, et al. Quantum cascade laser sensor for SO_2 and SO_3 for application to combustor exhaust streams[J]. Applied Optics, 2005, 44(31): 6635.
[23] Jiang J, Wang Z, Han X, et al. Multi-gas detection in power transformer oil based on tunable diode laser absorption spectrum [J]. IEEE Transactions on Dielectrics and Electrical Insulation, 2019, 26(1): 153-161.
[24] Hong X, Zhang C, Tian Y, et al. First TanSat CO_2 retrieval over land and ocean using both nadir and glint spectroscopy[J]. Remote Sensing of Environment, 2024, 304: 114053.
[25] Shen L, Jacob D J, Gautam R, et al. National quantifications of methane emissions from fuel exploitation using high resolution inversions of satellite observations[J]. Nature Communications, 2023, 14(1): 4948.
[26] Nugent-Glandorf L, Giorgetta F R, Diddams S A. Open-air, broad-bandwidth trace gas sensing with a mid-infrared optical frequency comb[J]. Applied Physics B, 2015, 119(2): 327-338.
[27] Gu M, Chen J, Mei J, et al. Open-path anti-pollution multi-pass cell-based TDLAS sensor for the online measurement of atmospheric H_2O and CO_2 fluxes[J]. Optics Express, 2022, 30(24): 43961.
[28] Pushkarsky M B, Webber M E, Baghdassarian O, et al. Laser-based photoacoustic ammonia sensors for industrial applications [J]. Applied Physics B: Lasers and Optics, 2002, 75(2-3): 391-396.
[29] Vincent T A, Gardner J W. A low cost MEMS based NDIR system for the monitoring of carbon dioxide in breath analysis at ppm levels [J]. Sensors and Actuators B: Chemical, 2016, 236: 954-964.
[30] Engelbrecht R. A compact NIR fiber-optic diode laser spectrometer for CO and CO_2:[J]. Spectrochimica Acta Part A: Molecular and Biomolecular Spectroscopy, 2004, 60(14): 3291-3298.
[31] Patterson C S, McMillan L C, Longbottom C, et al. Portable optical spectroscopy for accurate analysis of ethane in exhaled breath [J]. Measurement Science and Technology, 2007, 18(5): 1459-1464.
[32] Frodl R, Tille T. A high-precision NDIR CO_2 gas sensor for automotive applications[J]. IEEE Sensors Journal, 2006, 6(6): 1697-1705.
[33] Mizaikoff B. Waveguide-enhanced mid-infrared chem/bio sensors[J]. Chemical Society Reviews, 2013, 42(22): 8683.
[34] Lochbaum A, Dorodnyy A, Koch U, et al. Compact mid-infrared gas sensing enabled by an all-metamaterial design[J]. Nano Letters, 2020, 20(6): 4169-4176.
[35] Bareza N, Gopalan K K, Alani R, et al. Mid-infrared gas sensing using graphene plasmons tuned by reversible chemical doping [J]. ACS Photonics, 2020, 7(4): 879-884.
[36] Zheng K, Liao H, Han F, et al. Suspended waveguide-enhanced near-infrared photothermal spectroscopy for ppb-level molecular gas sensing on a chalcogenide chip[J]. Light: Science & Applications, 2026, 15(1): 116.
[37] Sonnenfroh D M, Allen M G. Absorption measurements of the second overtone band of NO in ambient and combustion gases with a 1.8-μm room-temperature diode laser [J]. Applied Optics, 1997, 36(30): 7970.
[38] Reid J, El-Sherbiny M, Garside B K, et al. Sensitivity limits of a tunable diode laser spectrometer, with application to the detection of NO_2 at the 100-ppt level [J]. Applied Optics, 1980, 19(19): 3349.
[39] Ngai A K Y, Persijn S T, Von Basum G, et al. Automatically tunable continuous-wave optical parametric oscillator for high-resolution spectroscopy and sensitive trace-gas detection [J]. Applied Physics B, 2006, 85(2-3): 173-180.
[40] Lancaster D G, Richter D, Curl R F, et al. Real-time measurements of trace gases using a compact difference-frequency-based sensor operating at 3.5 μm [J]. Applied Physics B: Lasers and Optics, 1998, 67(3): 339-345.
[41] Kasyutich V L, Holdsworth R J, Martin P A. Mid-infrared laser absorption spectrometers based upon all-diode laser difference frequency generation and a room temperature quantum cascade laser for the detection of CO, N_2O and NO[J]. Applied Physics B, 2008, 92(2): 271-279.
[42] Kasyutich V L, Martin P A. Multipass optical cell based upon two cylindrical mirrors for tunable diode laser absorption spectroscopy[J]. Applied Physics B, 2007, 88(1): 125-130.
[43] He Y, Orr B J. Rapid measurement of cavity ringdown absorption spectra with a swept-frequency laser [J]. Applied Physics B, 2004, 79(8): 941-945.
[44] Kasyutich V L, Canosa-Mas C E, Pfrang C, et al. Off-axis continuous-wave cavity-enhanced absorption spectroscopy of narrow-band and broadband absorbers using red diode lasers [J]. Applied Physics B: Lasers and Optics, 2002, 75(6-7): 755-761.
[45] Barry H R, Corner L, Hancock G, et al. Cavity-enhanced absorption spectroscopy of methane at 1.73 μm [J]. Chemical Physics Letters, 2001, 333(3-4): 285-289.
[46] Sonnenfroh D M, Rawlins W T, Allen M G, et al. Application of balanced detection to absorption measurements of trace gases with room-temperature, quasi-cw quantum-cascade lasers [J]. Applied Optics, 2001, 40(6): 812.
[47] McManus J B, Nelson D D, Herndon S C, et al. Comparison of cw and pulsed operation with a TE-cooled quantum cascade infrared laser for detection of nitric oxide at 1900 cm^{-1}[J]. Applied Physics B, 2006, 85(2-3): 235-241.
[48] Zhu Long-Hai, Duan Shi-Kun, Chen Mao-Hua, et al. Mid-wavelength infrared detector array based on black phosphorus ink thin film[J]. J. Infrared Millim. Waves, 2026, 45(3): 345-356.
(朱龙海,段世坤,陈茂华,等. 基于黑磷油墨薄膜的中波红外探测器阵列[J]. 红外与毫米波学报),2026, 45(3): 345-356.
[49] Parameswaran K R, Rosen D I, Allen M G, et al. Off-axis integrated cavity output spectroscopy with a mid-infrared interband cascade laser for real-time breath ethane measurements[J]. Applied Optics, 2009, 48(4): B73.
[50] Dahnke H, Von Basum G, Kleinermanns K, et al. Rapid formaldehyde monitoring in ambient air by means of mid-infrared cavity leak-out spectroscopy[J]. Applied Physics B: Lasers and Optics, 2002, 75(2-3): 311-316.
[51] Angelmahr M, Miklós A, Hess P. Photoacoustic spectroscopy of formaldehyde with tunable laser radiation at the parts per billion level[J]. Applied Physics B, 2006, 85(2-3): 285-288.
[52] Sun Q, Liu T, Yu X, et al. Non-interference NDIR detection method for mixed gases based on differential elimination [J]. Sensors and Actuators B: Chemical, 2023, 390: 133901.
[53] Végh P, Gulyás G, Huszár H, et al. Compensation of composition variation-induced sensitivity changes in gas phase photoacoustics [J]. Infrared Physics & Technology, 2024, 137: 105116.
[54] Weibring P, Richter D, Fried A, et al. Ultra-high-precision mid-IR spectrometer II: system description and spectroscopic performance[J]. Applied Physics B, 2006, 85(2-3): 207-218.
[55] Lewicki R, Wysocki G, Kosterev A A, et al. Carbon dioxide and ammonia detection using 2 μm diode laser based quartz-enhanced photoacoustic spectroscopy [J]. Applied Physics B, 2007, 87(1): 157-162.
[56] Koskinen V, Fonsen J, Roth K, et al. Cantilever enhanced photoacoustic detection of carbon dioxide using a tunable diode laser source[J]. Applied Physics B, 2007, 86(3): 451-454.

[57] Horstjann M, Bakhirkin Y A, Kosterev A A, et al. Formaldehyde sensor using interband cascade laser based quartz-enhanced photoacoustic spectroscopy [J]. Applied Physics B, 2004, 79 (7): 799-803.
[58] Yao C, Wang Q, Lin Y, et al. Photothermal CO detection in a hollow-core negative curvature fiber [J]. Optics Letters, 2019, 44 (16): 4048.
[59] Qi L, Chen W, Qiao S, et al. Mid-infrared quasi-distributed carbon monoxide gas sensing based on QEPAS and hollow waveguide[J]. Infrared Physics & Technology, 2025, 145: 105653.
[60] Mao X, Ye H, Tan Y, et al. High sensitivity miniaturized multipass absorption enhanced differential Helmholtz photoacoustic gas sensor [J]. Infrared Physics & Technology, 2024, 137: 105142.
[61] Zeng Yi-Hang, Xing Cheng-Zhi, Hai Guang-Yin, et al. A CO_2 retrieval algorithm for low-resolution spectrum [J]. J. Infrared Millim. Waves, 2026, 45(5):
(曾一航,邢成志,海光银,等. 基于低分辨率光谱的二氧化碳反演算法研究[J]. 红外与毫米波学报),2026, 45(5):.
[62] Meng J, Balendhran S, Sabri Y, et al. Smart mid-infrared metasurface microspectrometer gas sensing system [J]. Microsystems & Nanoengineering, 2024, 10(1): 74.
[63] Sun R, Li G, Yuan H, et al. A NDIR CO sensor enhanced by machine learning algorithm applying in gas outburst early warning [J]. Infrared Physics & Technology, 2025, 147: 105801.
[64] Lai L, Liu P, Zhou D, et al. Rapidly modulated wide-spectrum infrared source made of super aligned carbon nanotube film for greenhouse gas monitoring [J]. Advanced Functional Materials, 2023, 33(4): 2208891.
[65] Kim H, Uddin S Z, Lien D-H, et al. Actively variable-spectrum optoelectronics with black phosphorus [J]. Nature, 2021, 596 (7871): 232-237.
[66] Liu C, Wang G, Zhang C, et al. End-to-end methane gas detection algorithm based on transformer and multi-layer perceptron [J]. Optics Express, 2024, 32(1): 987.
[67] Liang Q, Bisht A, Scheck A, et al. Modulated ringdown comb interferometry for sensing of highly complex gases [J]. Nature, 2025, 638(8052): 941-948.
[68] Zhang S, Wu H, Liu S, et al. Rotating multi-channel high-sensitivity integrating sphere gas sensing based on NDIR [J]. Sensors and Actuators B: Chemical, 2025, 428: 137242.
[69] Chen Z, Zeng J, He M, et al. Portable ppb-level carbon dioxide sensor based on flexible hollow waveguide cell and mid-infrared spectroscopy [J]. Sensors and Actuators B: Chemical, 2022, 359: 131553.
[70] Jin W, Cao Y, Yang F, et al. Ultra-sensitive all-fibre photothermal spectroscopy with large dynamic range [J]. Nature Communications, 2015, 6(1): 6767.
[71] Zheng K, Peng Z, Liao H, et al. Dual slow-light enhanced photothermal gas spectroscopy on a silicon chip [J]. Nature Communications, 2025, 16(1): 10549.
[72] Xu X, Chen J, Wu H, et al. van der Waals complementary barrier infrared detector [J]. ACS Nano, 2025, 19 (19): 18747-18756.
[73] Yang Z, Bi Y-M, Wang Q, et al. Inflight performance of the TanSat atmospheric carbon dioxide grating spectrometer [J]. IEEE Transactions on Geoscience and Remote Sensing, 2020, 58(7): 4691-4703.
[74] Tan X, Zhang H, Li J, et al. Non-dispersive infrared multi-gas sensing via nanoantenna integrated narrowband detectors [J]. Nature Communications, 2020, 11(1): 5245.
[75] Sun H, Qiao S, He Y, et al. Parts-per-quadrillion level gas molecule detection: CO-LITES sensing [J]. Light: Science & Applications, 2025, 14(1): 180.
[76] Wu H, Zhang S, Qiao H, et al. An optical bandwidth optimization method for non-dispersive infrared gas sensors [J]. Sensors and Actuators B: Chemical, 2026, 448: 139035.
[77] Zifarelli A, Formica P, Sampaolo A, et al. Partial least squares regression analysis of natural gas-like mixtures absorption spectra collected using a mid-infrared supercontinuum broadband source[J]. Optics Express, 2025, 33(24): 50078.
[78] Yang Y, Wang Z, Wang P, et al. Robust gas species and concentration monitoring via cross-talk transformer with snapshot infrared spectral imager [J]. Sensors and Actuators B: Chemical, 2024, 413: 135780.
[79] Wan Z, Chen Y, Zhang X, et al. Quantum correlation-enhanced dual-comb spectroscopy [J]. Light: Science & Applications, 2025, 14(1): 257.
[80] Lin H, Zheng H, Zhu W, et al. Multifunctional lithium niobate platform for photodetection and photoacoustic and thermoelastic gas sensing[J]. Nature Communications, 2026, 17(1): 2296.

红外气体传感技术:从经典方法到新兴前沿

吴海涛[1,2,3], 杭 锐[1,3], 李 庆[1,2,3*], 胡伟达[1,2,3]
(1. 国科大杭州高等研究院 物理与光电工程学院,浙江 杭州 310024;
2. 中国科学院上海技术物理研究所 红外探测全国重点实验室,上海 200083;
3. 中国科学院大学,北京 100049)

摘要:红外气体传感基于气体分子的特征红外吸收,为气体成分识别和浓度定量提供了一种光学检测方法。该技术已广泛应用于环境监测、工业安全、呼气分析、遥感探测等领域。随着小型化、集成化和多组分检测系统需求的不断增长,红外气体传感器的性能已不再仅由单一器件优化决定,而是越来越依赖于光源、气室、探测器和光谱模型的协同设计。本文从系统级设计和关键使能技术的角度,总结了红外气体传感领域的最新进展。首先,讨论了光源从宽谱非相干热源向激光器和频率梳的演进;随后,综述了包括自由空间气室、空心光纤和片上波导在内的光学气室;接着,从光子型、热型以及光声检测机制等方面总结了探测器技术;此外,还讨论了用于信息提取的光谱建模方法,包括采样优化、多变量回归和机器学习。最后,展望了红外气体传感向高灵敏、多组分分析、小型化、智能化和片上集成方向发展的未来趋势。

关 键 词:红外气体传感;分子吸收光谱;器件集成;光谱建模;智能光谱反演
中图分类号:O43 **文献标识码**:A